JOURNAL OF ENERGY SYSTEMS

2023, 7(1)

2602-2052 DOI: 10.30521/jes.1160462 Research Article

Energy analysis of a small-scale multi-effect distillation system powered by photovoltaic and thermal collectors

Mahmoud Sheta*
Egypt-Japan University of Science and Technology (E-JUST), Energy Resources Engineering Department, Alexandria, Mansoura University, Mechanical Power Engineering Department, El-Mansoura, Egypt, Mahmoud.Sheta@ejust.edu.eg
Ahmed Elwardany
Egypt-Japan University of Science and Technology
Alexandria University, Mechanical Engineering Department, Alexandria, Egypt, ahmed.elwardany@ejust.edu.eg
Shinichi Ookawara
Tokyo Institute of Technology, Tokyo, Japan, ookawara.s.aa@m.titech.ac.jp
Hamdy Hassan
Egypt-Japan University of Science and Technology (E-JUST), Energy Resources Engineering Department, Alexandria
Assiut University, Mechanical Power Engineering Department, Assiut, Egypt, hamdy.aboali@ejust.edu.eg

Submitted: 10.08.2022
Accepted: 18.12.2022
Published: 31.03.2023

* *Corresponding Author*

Abstract: Powering thermal desalination technologies by renewable energy is believed to be a viable solution to overcome the worldwide freshwater scarcity problem without causing more damage to the environment. In this paper, a multi-effect distillation system (MED) with mechanical vapor compression is powered by the generated electrical power of photovoltaic/thermal collectors and assisted by the by-product thermal power generated. The system is sized according to thermal power needed and designed for small-scale application and weather conditions of Alexandria, Egypt. Excess electricity is injected into the grid and hot water storage tank is used as a back-up to compensate low and fluctuating radiation. Results show that, at a saturation temperature of MED's heating steam of 55 °C, freshwater production is 11.1 m3/day in 10 hours of operation, system specific power consumption is 9.72 kWh/m3, specific area is 317.04 m2s/kg, and performance ratios of the desalination unit is 3.33 and 6.97 for the overall system. However, at T = 65 °C the system's electrical energy is totally absorbed by the compressor, and the system's performance decreases.

Keywords: *Desalination, Multi-effect distillation, Performance, Photovoltaic, Solar Energy, Thermal*

Cite this paper as: Sheta, M., Elwardany, A., Ookawara, S., & Hassan, H., Energy analysis of a small-scale multi-effect distillation system powered by photovoltaic and thermal collectors. *Journal of Energy Systems 2023; 7*(1): 89-105, DOI: 10.30521/jes.1160462

Nomenclature

A	Heat transfer area, m2
G	Global radiation, W/m2
h	Enthalpy, kJ/kg
M	Mass flow rate, kg/s
Q	Heat, kW
r	Compression ratio
sA	Specific area, m2/kg
U	Heat transfer coefficient, W/m2.K
W	Work, kW
x	Dryness fraction

Abbreviations

BPE	Boiling point elevation, °C
LMTD	Logarithmic mean temperature difference, °C
MED	Multi-effect distillation
MVC	Mechanical vapor compression
NEA	Non-equilibrium allowance, °C
ORC	Organic Rankine cycle
PR	Performance ratio
SPC	Specific power consumption, kWh/m^3

Greek symbols

α	Fraction of vapor condensed in preheater
β	Power temperature coefficient %/°C

Subscripts

B	Brine
c	Condenser
D	Distillate
e	Effect
FB	flash box
FE	Flashing in Effect
fg	Latent heat
L	Saturated liquid
preh	Preheater
S	Steam
sat	Saturated vapor
ref	SW
T	Total
t	Tilted
V	Vapor

1. INTRODUCTION

The increasing world population and climate change have caused severe water shortage in many regions of the world specially in developing countries with limited natural water resources [1,2]. This situation is believed to get more complicated in the future as global warming is causing more drought each year. Although there are multiple desalination technologies, which are well established and reliable, their requirements of energy is high and the cost of their construction and operation is significant [3]. Reverse osmosis is one of the most common techniques of desalination which is widely used around the world [4]. However, it is not reliable for regions like Middle Eastern seas because of the harsh conditions and higher sea salinities. Thermal desalination technologies like multi-stage flash and multi-effect distillation are most suitable for these conditions. That is the cause of their dominance in regions like the Arab gulf countries [5]. The most serious concern about thermal technologies is their high demand of fossil fuel and consequently, damaging effect on nature [6]. The renewable sources of energy represent a promising solution to that problem especially solar energy which happens to be abundant in the same regions where drought is most prominent.

Literature is already rich in research on powering thermal desalination systems by solar energy which is an important trend in recent years. A multi-effect distillation system (MED) plant powered by 849 m^2 of evacuated tube solar collectors was studied by Kim *et al.,* [7]. They found that the annual collector efficiency decreases from 57.3% to 54.8% with an increase of the heating steam temperature from 80 °C to 90 °C. However, the overall water production rate increases from 0.18 kg/s to 0.21 kg/s and the performance ratio from 4.11 to 4.13 [7]. Liu et. al., theoretically studied another MED system powered by evacuated tube solar collectors. They investigated the effect of varying heating steam temperature of the first effect and number of effects on system performance. Their results showed that an increase in heating steam temperature or number of effects decreases water cost [8]. A solar trigeneration system producing electricity, freshwater, cooling, and heating effects was modelled by Calise and co-workers [9]. They used concentrated photovoltaic/thermal collectors as heat and electricity source, MED for desalination and absorption chiller for cooling and heating effects. In addition, they used a biomass-fired heater for powering the MED unit. The system was dynamically simulated to determine the optimum values for design parameters [9]. Alhaj *et al.,* [5] investigated the performance of an MED system coupled to linear Fresnel collectors with storage system and an air-cooled condenser. Their system produced 8.6 m^3 per m^2 of collector yearly and they managed to reduce the cost and the plant water consumption by 2 m^3 of seawater per m^3 of feed water. The concentrated photovoltaic/thermal collector was coupled to MED for simultaneous production of water, power and heating by Zhang *et al.,* [10]. The system was studied from energy and exergy perspectives. The results indicate that the system is performing better than individual systems combined. Alsehli *et al.,* [11] integrated parabolic trough solar collectors with MED and thermal storage tanks. The required collector area was calculated to be 92000 m^2 for a 2200 m^3 production of distilled water. The performance ratio was 2 and specific thermal energy consumption was 1140 kJ/kg [11]. Integrating low temperature MED with salinity gradient solar pond was studied by Parsa *et al.,* [12] economically for 200000 m^3/year of fresh water. Soliman *et al.* [13] compared the performance and cost of an MED system powered by large scale solar tower and parabolic trough collectors combined with ORC against Rankine cycle, ORC proved better. A hybrid desalination system implementing reverse osmosis and MED together was organic Rankine cycle that is supplied with solar power using a parabolic trough solar collector was modelled by Naminezhad *et al.,* [14]. The different organic fluids were used as working media for the Rankine cycle. They found that n-octane had the highest rate of freshwater production and lowest exergy destruction.

Despite the vast interest in the topic, matching the thermal and electrical requirements of MED with a low-temperature, commercial and non-concentrated photovoltaic/thermal collectors for small-scale applications have not been presented, yet. In this paper, a small-scale multi-effect distillation with mechanical vapor compression unit (MVC) is powered by PVT solar collectors for simultaneous

production of freshwater. Energy analysis is performed, the system efficiency is investigated, and the overall system is tested under the climate conditions of Alexandria, Egypt. First, the main features of the system are demonstrated. Then, a mathematical model is presented and solved for system's performance parameters. System performance is evaluated and main key results are discussed. Finally, the system is tested and overall key observations are recorded.

2. SYSTEM DESCRIPTION

The proposed system layout is presented in Fig. 1. A solar field of photovoltaic/thermal collector produces both heat and electricity [15]. The thermal energy is delivered to water storage tanks while the electrical energy is used to power the system components and the rest is injected into the grid. The storage tanks are used to provide thermal energy for extended hours of operation and at the same time accommodate weather changes. A flash separator is used to produce the vapor required by the distillation unit but at a lower pressure. The small scale multi-effect distillation with mechanical vapor compression (MED-MVC) desalination unit design and arrangement is based on Ref. [16] with a modification of adding the compressor. The unit is designed to produce only 10 m^3/day of fresh water in 9 hours of operation and is composed of 4 effects. The compressor elevates the pressure and temperature of that vapor giving it the ability to assist in the unit operation which saves a portion of the electrical energy required by the system. The superheated vapor at the outlet of the compressor is sent to the first effect to evaporate a quantity of the preheated feed seawater. Some of that quantity is condensed in the preheater and the rest is sent to the following effect. The process is repeated as each effect is at a pressure and temperature lower than the previous effect to permit evaporation by both boiling and flashing. The condenser is used in the original system by Delgado *et al.*, [16] to condense the total amount of last effect's steam, but here it is reduced and used as a preheater. A ratio of the total freshwater produced is directed back to the solar circuit for mass conservation while the rest is extracted and bottled.

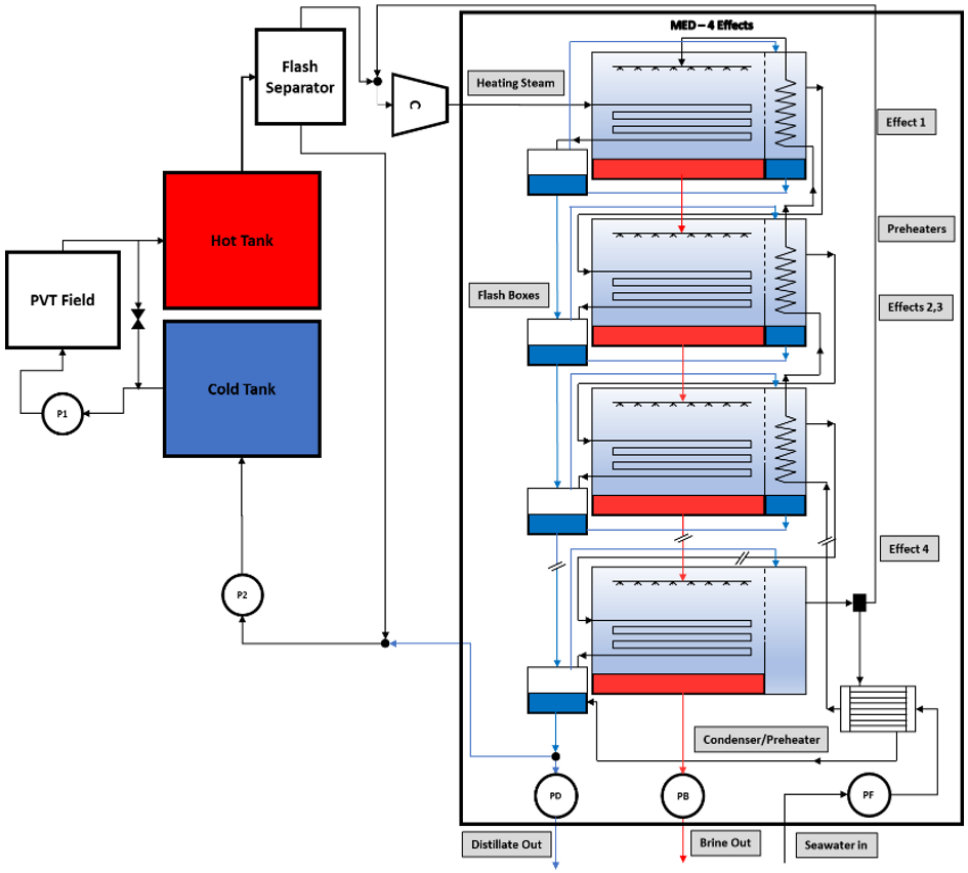

Figure 1. The system layout

3. MATHEMATICAL MODEL

3.1 MED-MVC Subsystem

In this paper, a simplified forward feed multi-effect distillation model is built on the detailed model by Delgado *et al.*, [16] with the assumptions and following approximations:

No thermal losses considered, no saturation temperature loss in demisters and connecting pipes, no leaks in the system due to vacuum, distillate is salt free, inlets and outlet effects' streams are at saturation conditions except first effect, boiling point elevation and non-equilibrium allowance are considered, flash boxes temperatures are equal to effect's vapor saturation temperatures, heat transfer areas for effects and preheaters are taken as equal for economic measures, pumping requirements neglected and finally seawater properties are based on a library by Sharqawy *et al.*, [17,18].

The model is generated by applying mass, salinity, energy balances in addition to heat transfer equations to all the effects, flash boxes, preheaters, and condenser.

3.1.1 Effect 1

Feed seawater enters the first effect after getting preheated. The superheated steam coming from the compressor raises its temperature to effect's temperature at which boiling starts and the heating steam condenses and moves to the flash box. The flash box is at lower pressure than heating steam, that's why flashing occurs, and the generated vapor is sent back to the effect. A portion of each effect's vapor will condense in the preheater to provide preheating for better overall performance of the system. This generated vapor in the first effect will be the heat source for the following effect as it will be at a lower pressure and consequently water evaporates at a lower temperature. The mass and salinity balances on the effect and flash box are given by,

$$M_F + M_{VFB,1} = M_{T,1} + M_{Bout,1}, \quad (1)$$

$$M_{T,1} = M_{D,1} + M_{VFB,1}, \quad (2)$$

$$M_S + \alpha_1 M_{T,1} = M_{VFB,1} + M_{FB,1}, \quad (3)$$

$$M_F\, X_{in} = M_{Bout,1}\, X_{out,1}, \quad (4)$$

where the flow rates; M_F for the feed seawater, $M_{VFB}$for the flashed vapor from flash box, M_T for the total amount of vapor, M_D for the portion of vapor generated by boiling, M_S for the heating steam supplied to unit, $M_{FB}$for the distillate out of the flash box, M_{Bout} for brine out of the effect whereas α is the ratio of vapor to be condensed in the preheater and X is the salinity.

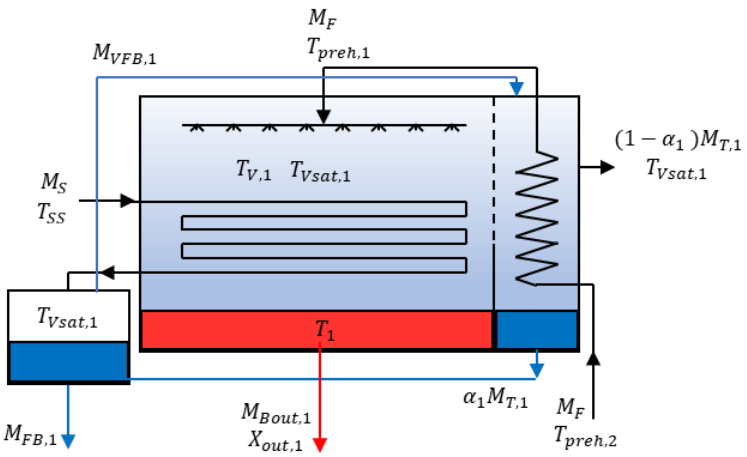

Figure 2. The sketch of Effect 1.

Energy balance on the effect, flash box and preheater are given by,

$$M_S\left(h_{Sup,S}-h_{Sat,S}\right)+M_S h_{fg,S}+M_F h_{preh,2}+M_{VFB,1}h_{V,1}=(1-\alpha_1)M_{T,1}h_{V,1}+\alpha_1 M_{T,1}h_{L,1}+M_{Bout,1}h_{Bout,1}\,, \quad (5)$$

$$M_S h_{L,S}+\alpha_1 M_{T,1}h_{L,1}=M_{VFB,1}h_{V,1}+M_{FB,1}h_{L,1}, \quad (6)$$

$$M_F C_{ppreh,1}\left(T_{preh,1}-T_{preh,2}\right)=\alpha_1 M_{T,1}h_{fg,1}. \quad (7)$$

where $h_{Sup,S}, h_{Sat,S}, h_{fg,S}$ are enthalpies of superheated heated steam at temperature T_{SS}, saturated heated steam at temperature T_S and its latent heat of condensation, respectively. $h_V, h_L, h_{\mathrm{fg}}$ are enthalpies of the effect's saturated vapor, liquid and latent heat, respectively. The effect temperatures are given by,

$$T_1=T_{Vsat,1}+BPE_1, \quad (8)$$

$$T_{V,1}=T_1. \quad (9)$$

The boiling point elevation, BPE, is the increase in boiling point of seawater due to its salinity [17]. T_V is the vapor actual temperature in the effect. However, only saturation temperature is considered for simplicity as the superheat portion is negligible if compared to the latent heat.

3.1.2 Effects 2 and 3

Effects include a flashing process as brine at saturated condition following the first effect. They enter them and the system is exposed to a lower pressure. The flow rate of the generated amount is $M_{VFE,i}$

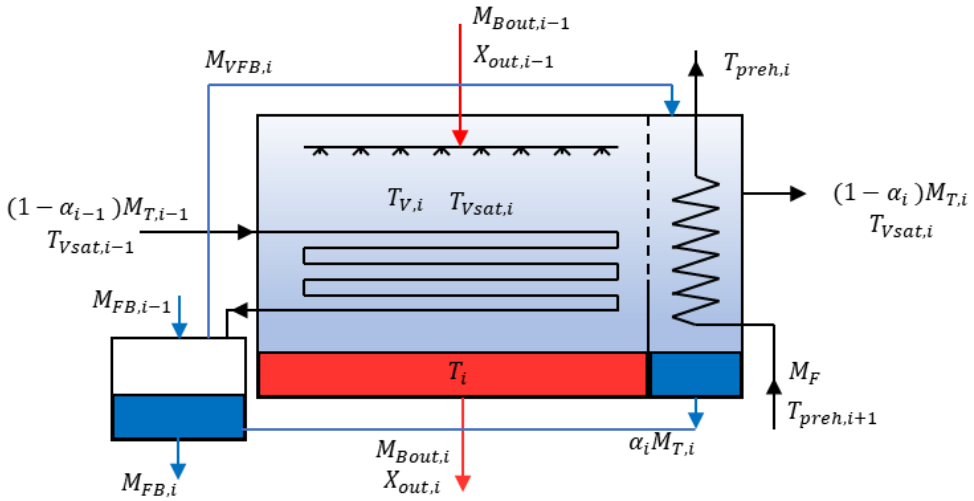

Figure 3. The sketch of Effect I, where i =2,3.

Mass and salinity balances on effect and flash box are stated as follows:

$$M_{Bout,i-1}+M_{VFB,i}=M_{T,i}+M_{Bout,i}, \quad (10)$$

$$M_{T,i}=M_{D,i}+M_{VFB,i}+M_{VFE,i}, \quad (11)$$

$$(1-\alpha_{i-1})M_{T,i-1}+M_{FB,i-1}+\alpha_i M_{T,i}=M_{VFB,i}+M_{FB,i}, \quad (12)$$

$$M_{Bout,i-1}\,X_{out,i-1}=M_{Bout,i}\,X_{out,i}. \quad (13)$$

The energy balance on the effect, flash box and preheater are given by,

$$\begin{aligned}(1-\alpha_{i-1})M_{T,i-1}h_{fg,i-1}+M_{VFB,i}h_{V,i}+M_{Bout,i-1}h_{Bout,i-1}\\ =(1-\alpha_i)M_{T,i}h_{V,i}+\alpha_i M_{T,i}h_{L,i}\\ +M_{Bout,i}h_{Bout,i}+M_F C_{ppreh,i}\left(T_{preh,i}-T_{preh,i+1}\right),\end{aligned} \quad (14)$$

$$(1-\alpha_{i-1})M_{T,i-1}h_{L,i-1}+M_{FB,i-1}h_{L,i-1}+\alpha_i M_{T,i}h_{L,i}=M_{VFB,i}h_{V,i}+M_{FB,i}h_{L,i}, \quad (15)$$

$$M_F C_{ppreh,i}\left(T_{preh,i}-T_{preh,i+1}\right)=\alpha_i M_{T,i}h_{fg,i}. \quad (16)$$

Effect temperatures are given as follows:

$$T_i=T_{Vsat,i}+BPE_i, \quad (17)$$

$$T_{V,i}=T_i, \quad (18)$$

$$T_{FE,i}=T_i+NEA_i, \quad (19)$$

$$NEA_i=\frac{33(\Delta T_i)^{0.55}}{T_{V,i}}, \quad (20)$$

where $T_{FE,i}$ is the temperature of brine directly at the effect's inlet due to the flashing process and it is higher than the effect's temperature by the non-equilibrium allowance NEA_i [19]. ΔT_i is the temperature difference between two successive effects.

The flash process is stated as,

$$M_{VFE,i}h_{fgSW,i}=M_{Bout,i-1}C_{pFE,i}(T_{i-1}-T_{FE,i}), \quad (21)$$

where $h_{fgSW,i}$ is the latent heat of seawater, $C_{pFE,i}$ is the specific heat capacity of seawater at the average temperature between $T_{i-1}$and $T_{FE,i}$.

3.1.3 Effect 4 and Condenser

In the model introduced by Delgado *et al.*, [16], the last effect does not include a preheater as the condenser will act as one, beside condensing last effect's steam. Here the condenser is reduced and used as a preheater as most steam will be redirected to the compressor. The mass and salinity balances on the effect, flash box and condenser are as following:

$$M_{Bout,3}+M_{VFB,4}=(1-\alpha_4)M_{T,4}+M_{Bout,4}, \quad (22)$$

$$M_{T,4}=M_{D,4}+M_{VFB,4}+M_{VFE,4}, \quad (23)$$

$$(1-\alpha_3)M_{T,3}+M_{FB,3}+M_{V,Cond}=M_{VFB,4}+M_{FB,4}, \quad (24)$$

$$M_{Bout,3}\,X_{out,3}=M_{Bout,4}\,X_{out,4}, \quad (25)$$

$$M_{V,Comp}=(1-\alpha_4)M_{T,4}-M_{V,Cond}, \quad (26)$$

$$M_{Cycle} = M_{FB,4} - M_{Dist}, \tag{27}$$

where $M_{V,Comp}$ is the amount of steam redirected back to the compressor, $M_{V,Cond}$ is the amount condensed and used for preheating in the condenser. M_{Cycle} is the amount of freshwater sent back to the solar cycle for mass conservation and M_{Dist} is the extracted useful amount. The energy balance on the effect, flash box and condenser are explained by,

$$\begin{aligned}(1-\alpha_3)M_{T,3}h_{fg,3} + M_{VFB,4}h_{v,4} + M_{Bout,3}h_{Bout,3} \\ = M_{T,4}h_{V,4} + M_{Bout,4}h_{Bout,4},\end{aligned} \tag{28}$$

$$(1-\alpha_3)M_{T,3}h_{L,3} + M_{FB,3}h_{L,3} + M_{V,Cond}h_{L,4} = M_{VFB,4}h_{V,4} + M_{FB,4}h_{L,4}, \tag{29}$$

$$M_{V,Cond}h_{fg,4} = M_F C_{p,SWin}(T_F - T_{SW,in}). \tag{30}$$

The effect temperatures are given by,

$$T_4 = T_{Vsat,4} + BPE_4, \tag{31}$$

$$T_{V,4} = T_4, \tag{32}$$

$$T_{FE,4} = T_4 + NEA_4, \tag{33}$$

$$NEA_4 = \frac{33(\Delta T_4)^{0.55}}{T_{V,4}}. \tag{34}$$

The flash process is defined by,

$$M_{VFE,4}h_{fgSW,4} = M_{Bout,3}C_{pFE,4}(T_3 - T_{FE,4}). \tag{35}$$

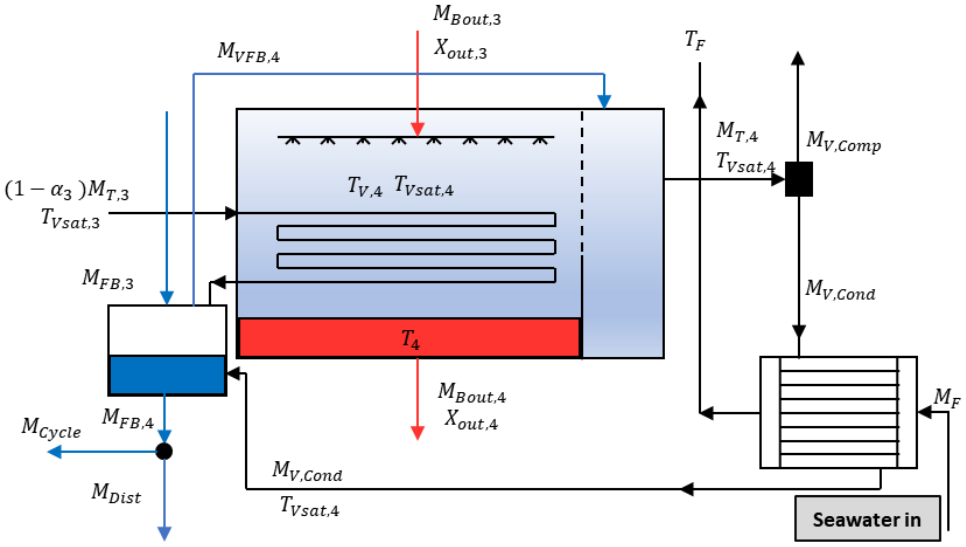

Figure 4. The sketch of Effect 4 and the condenser.

The heat transfer equations for the effects, preheaters and condenser are defined as following. The overall heat transfer coefficient for the effects following Ref. [20] is given by,

$$\begin{aligned}U_{e,i} = 1.9695 + 1.2057x10^{-2}T_i - 8.5989x10^{-5}T_i^2 \\ +2.5651x10^{-7}T_i^3.\end{aligned} \tag{36}$$

The overall heat transfer coefficient for the condenser after Ref. [20] and for the preheaters after Ref. [16] are as follows,

$$U_c = 1.7194 + 3.2063x10^{-3}T_{Vsat,4} + 1.5971x10^{-5}T_{Vsat,4}^2 - 1.9918x10^{-7}T_{Vsat,4}^3. \quad (37)$$

Effect 1 is defined as,

$$Q_1 = A_1 U_{e,1}(T_s - T_1). \quad (38)$$

Effects 2:4 are defined as,

$$Q_i = A_i U_{\mathrm{e,i}}\left(T_{Vsat,i-1} - T_i\right). \quad (39)$$

Preheaters 1:3 are defined as,

$$Q_{preh,i} = A_{preh,i}U_{preh,i}\mathrm{LMTD}_{preh,i} = U_{preh,i}A_{preh,i}\frac{T_{preh,i} - T_{preh,i+1}}{\ln\left(\frac{T_{\mathrm{Vsat,i}} - T_{preh,i+1}}{T_{\mathrm{Vsat,i}} - T_{preh,i}}\right)}. \quad (40)$$

Condenser definition is given by,

$$Q_c = A_c U_c \mathrm{LMTD}_c = U_c A_c \frac{T_F - T_{SW,in}}{\ln\left(\frac{T_{Vsat,4} - T_{SW,in}}{T_{Vsat,4} - T_F}\right)}. \quad (41)$$

The compressor work is defined by,

$$W_{Comp} = (M_{V,Comp} + M_{V,Solar})(h_{Sup,S} - h_{v,4}), \quad (42)$$

$$r_{Comp} = \frac{P_{sat\ at\ T_S}}{P_{sat\ at\ T_{Vsat,4}}}, \quad (43)$$

where $M_{V,Solar}$ is the amount of steam provided through the solar field, $h_{Sup,S}$ is the actual enthalpy at compressor outlet, $h_{\mathrm{v},4}$ is the enthalpy of redirected steam from last effect and the solar field.

$$M_S = M_{V,Comp} + M_{V,Solar}, \quad (44)$$

where M_S is the total heating steam flow rate. The MED-MVC performance parameters are given by,

$$\mathrm{sA} = \frac{\sum_{i=1}^{4} A_i + \sum_{i=1}^{3} A_{\mathrm{preh},i} + A_c}{M_{Dist}}. \quad (45)$$

Here, sA is the specific area in m^2/kg_{Dist} and it is used to compare systems of different features as it is a measure of how much heat transfer area is required and consequently, the cost.

$$SPC = \frac{W_{\mathrm{Comp}}}{M_{\mathrm{Dist}}} * \frac{1000}{3600} \quad (46)$$

The SPC is the specific power consumption in kWh/m^3 and given by,

$$PR_{\mathrm{MED-MVC}} = \frac{M_{\mathrm{Dist}} h_{\mathrm{fg},4}}{M_s h_{\mathrm{fg},s} + W_{\mathrm{Comp}}/\eta_{thermal}}. \quad (47)$$

$PR_{\mathrm{MED-MVC}}$ is the performance ratio [21] and η_{thermal} is average thermal power stations efficiency which is used here to give a better indication by transforming high grade electricity into primary energy [22,23].

3.2 Storage Tanks and Flash Box

The flash box is used to generate low pressure and temperature steam to assist in MED-MVC operation. First, the required output amount is calculated from MED-MVC solution, $M_{V,Solar}$, then flash box input flow rate is specified. The flash box is kept at a pressure equal to last effect's pressure. The formulation is given by,

$$x = \frac{h_{flash,in} - h_{L,out}}{h_{V,out} - h_{L,out}}, \quad (48)$$

$$M_{HotWater} = M_{V,Solar}/x, \quad (49)$$

where $M_{HotWater}$ is the required flowrate from the hot water tank and x is the ratio of output vapor to the inlet flow rate.

The hot water tank is designed to provide constant flow rate and keep the system working for a specified number of days in addition to compensating for fluctuating solar radiation. The capacity of the tank is calculated as follows,

$$E_{Tank} = Q_{PVT} N_{hrs/day} N_{days}\ 1000 \text{ x } 3600, \quad (50)$$

$$m_{Tank} = E_{Tank}/(C_p(T_{HotTank} - T_{ColdTank})), \quad (51)$$

where Q_{PVT} is the required solar thermal power in kW, $T_{ColdTank}$, $T_{HotTank}$ are fixed temperatures and m_{Tank} is the total hot water amount in the hot tank in kg.

3.3 PVT Solar Field

A simplified model is implemented to find the main output parameters of the PVT panels with simplifying assumptions following Ref. [24]. The electricity production from Ref. [25] is given by,

$$\eta_{electrical} = \eta_{nominal}[1 - \beta(T_{PVT} - T_{S.C.})], \quad (52)$$

$$P_{electrical} = \eta_{electrical} * G_t * A_{PVT}, \quad (53)$$

where $\eta_{nominal}$ is the nominal electrical efficiency at standard conditions of $G_t = 1000$ W/m^2 and $T_{S.C.} = 25$ °C, parallel with Ref. [26], β is the power temperature coefficient which accounts for the decrease in efficiency due to higher temperatures. T_{PVT} is the panel surface temperature. Thermal energy balance is defined as,

$$\eta_{thermal} G_t A_{PVT} = \dot{m}_W c_{P,W}(T_{W,out} - T_{W,in}), \quad (54)$$

$$P_{ele,net} = P_{electrical} - W_{Comp}, \quad (55)$$

where $\eta_{thermal}$ is the thermal efficiency, a_0 is the optical efficiency, a_1, a_2 are heat loss coefficients which are different for each PVT model, $T_{W,AVG}$ is the average temperature of the cooling water in and out, T_{sur} is the surrounding temperature. PR_{Overall} is the system overall performance ratio calculated the same way as Eq. (47):

$$PR_{\text{Overall}} = \frac{M_{\text{Dist}} h_{\text{fg},4} + P_{\text{ele,net}}/\eta_{thermal}}{P_{Solar}} \tag{56}$$

The mathematical model is a set of non-linear equations that is solved using MatLab. First, the model is solved for the design point. Then, overall system performance changes with changing main parameters are investigated.

4. RESULTS AND DISCUSSION

4.1 Model Validation

The main MED model is validated against that one by Delgado *et al.*, [16] in Table 1, with the same layout and arrangement and same input conditions of the following: Distillate output 1 kg/s, input steam is saturated at 70 °C, inlet seawater temperature is 25 °C, inlet salinity is 42000 ppm, output salinity is 70000 ppm, last effect's temperature is 40 °C, terminal temperature difference in the first preheater is 5 °C, and increase in temperature across condenser is 10 °C.

Further simplifications are considered as follows: No pressure or saturation temperature losses in the demister and connecting lines, the superheat portion is neglected in the effects and preheaters. In addition, only 4 effects are studied, which is suitable for small-scale applications. Validation is presented in Table 1. An acceptable agreement is fulfilled. The combined MED-MVC system was tested for the validation with 63.36 m^3/h distillate production and 62.5 °C heating steam temperature. The calculated performance ratio is 3.1744, which is comparable to 3.19 according to the study of Elsayed *et al.*, [22]. The specific power consumption of the 2 effect MVC with makeup steam by Ref. [21] is 9.4 kWh/m^3 which is close to the 9.7 kWh/m^3 for 4 effects here at 55 °C heating steam saturation temperature.

Table 1. The validation.

	4 Effects (after [16])	Present Model	% Error
GOR	3.543	3.520	0.649
sA	189.130	188.480	0.344
$\Delta T_{1,2}$	7.040	7.255	3.054
$\Delta T_{2,3}$	7.126	7.277	2.119
$\Delta T_{3,4}$	7.237	7.366	1.783
$\Delta T_{\text{preh }1,2}$	7.222	7.369	2.035
$\Delta T_{\text{preh }2,3}$	7.370	7.339	0.421
$\Delta T_{\text{preh }3,\text{cond}}$	7.592	7.189	5.308
α_1	0.118	0.124	5.085
α_2	0.121	0.126	4.132
α_3	0.125	0.126	0.800
$TTD_{\text{preh},2}$	5.182	5.000	0.000
$TTD_{\text{preh},3}$	5.429	5.114	1.312
$M_{D,1}$	0.259	5.176	4.660
$M_{D,2}$	0.233	0.262	1.158
$M_{D,3}$	0.229	0.233	0.000
$M_{D,4}$	0.226	0.227	0.873

4.2 Input Data

The solar radiation data for Alexandria, Egypt are collected from Meteonorm software. The annual average global radiation on 30° inclined surface for that location is 622 W/m^2 and average sunshine hours is 8.99 hrs. These values are used as a design point. A commercial PVT model from DualSun, France is used with characteristics presented in Table 2. Solar field sizing is based on the thermal energy requirements of the desalination unit. No consideration has been given to electrical load as the system is connected to the grid and the main purpose is to recover low grade heat.

Table 2. PVT model characteristics.

Electrical		**Thermal**		
Nominal power	400 W	Thermal power	660 W_{th}/m²	
Module efficiency	21.3 %	Collector area	1,876 m²	
Power temperature coefficient	-0.34 %/°K		Non-insulated	Insulated
		Stagnation temperature	80°C	90°C
		Optical efficiency a_0	63.3 %	62.1 %
		Coefficient a_1	11.5 W/K/m²	7.4 W/K/m²
		Coefficient a_2	0 W/(m².K²)	0 W/(m².K²)

The following input data are applied: For the MED-MVC, distillate output is fixed at 10 m^3/day in 9 hours of operation, seawater inlet temperature and salinity are 25 °C and 42000 ppm, respectively. The last effect's temperature and salinity are 40 °C and 70000 ppm, respectively. In addition, the compressor efficiency is assumed to be 90% in this respect. The flash box saturation temperature is made equal to last effect's temperature. Hot water storage tank is designed to provide energy for 2 days with no solar power input. Its temperature is fixed at 55 °C which is suitable for the chosen PVT model, cold tank temperature is fixed at flash box temperature. The PVT model is assumed to provide a fixed temperature of 55 °C by changing the water flowrate.

4.3 System Power

Fig. 5 shows that the required solar thermal energy is 39.166 kW, which is more than 3 times the compressor power at T=55 °C. The solar field is sized according to the required thermal power and the compressor power at this design point is taking up 50.9% of the generated electric power of the PVT field. At this point, the portion of the solar vapor is almost 20% of the total heating steam. Elevating the temperature to 60 °C decreases the required thermal power by 6.3% due to the decline in the required solar vapor flowrate, and increases compressor work by 33.6%. This large jump causes the power consumption to increase by 21.7% to reach a value of 72.6% of the total electric power of the filed. The same trend keeps going until a maximum point is reached at 65 °C, where the produced solar electric power is nearly sufficient to power the compressor with no extra production.

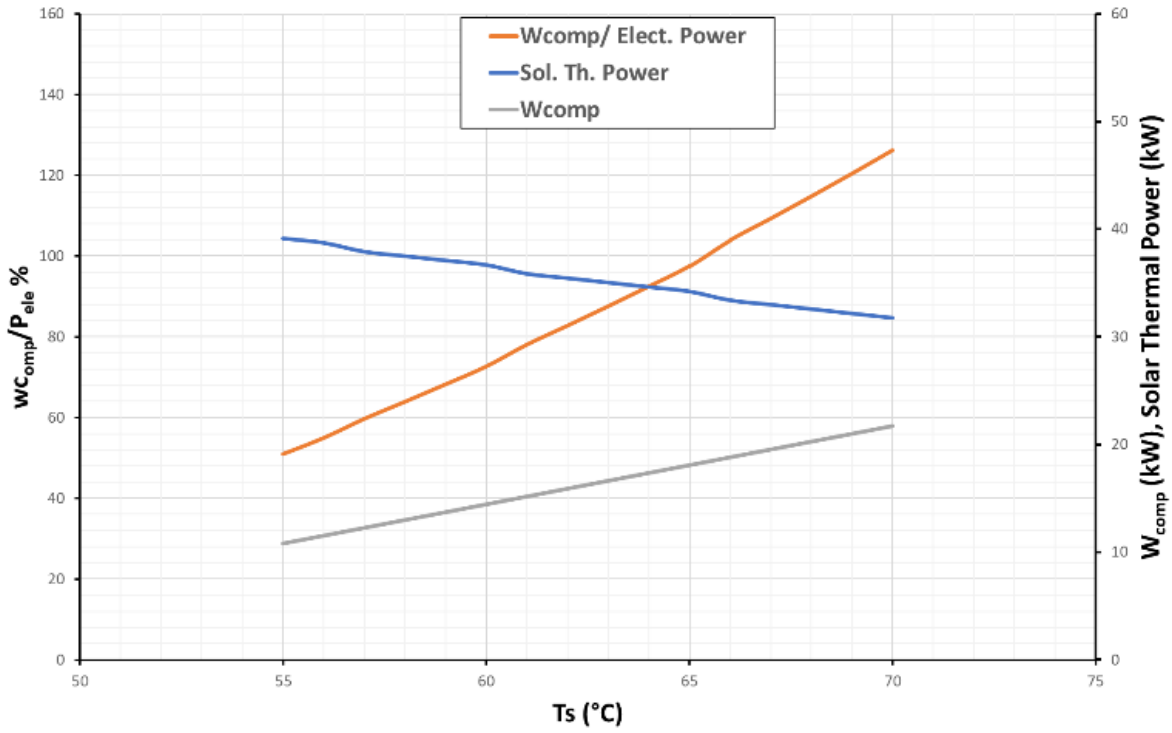

Figure 5. Compressor power, solar thermal and electrical power changes with temperature.

This happens because the increase in saturation temperature increases the pressure ratio of the compressor and consequently, power consumption. At the same time, the flowrate of the solar vapor required decreases due to more vapor being generated inside effects and same amount of distillate is extracted (Fig. 6).

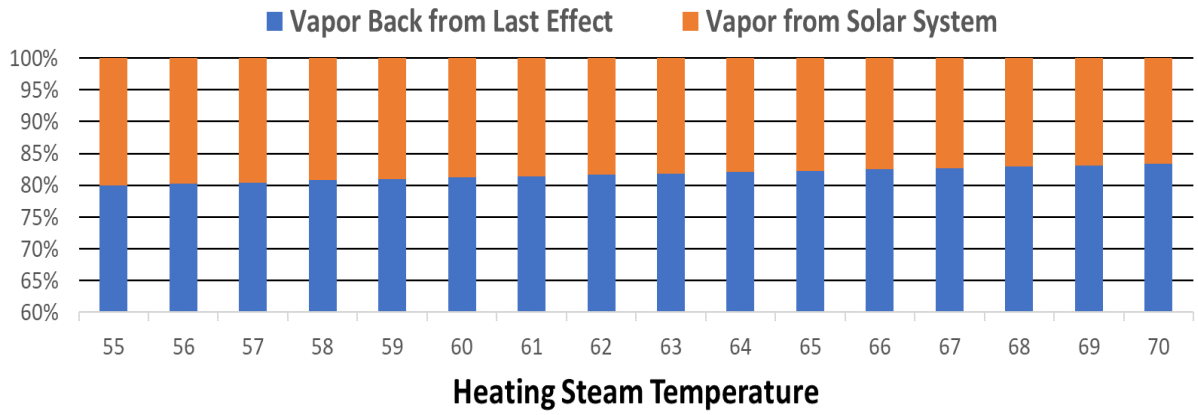

Figure 6. Vapor from solar system against vapor from last effect at the inlet of the compressor.

4.4 System Performance

Lower temperature operation means that higher specific area is required and consequently the system initial cost would be higher. On the other hand, lower temperatures result in lower specific energy consumption and lower operating costs. As shown in Fig. 7, rising the temperature from 55 °C to 70 °C nearly halves the specific area and doubles specific power consumption.

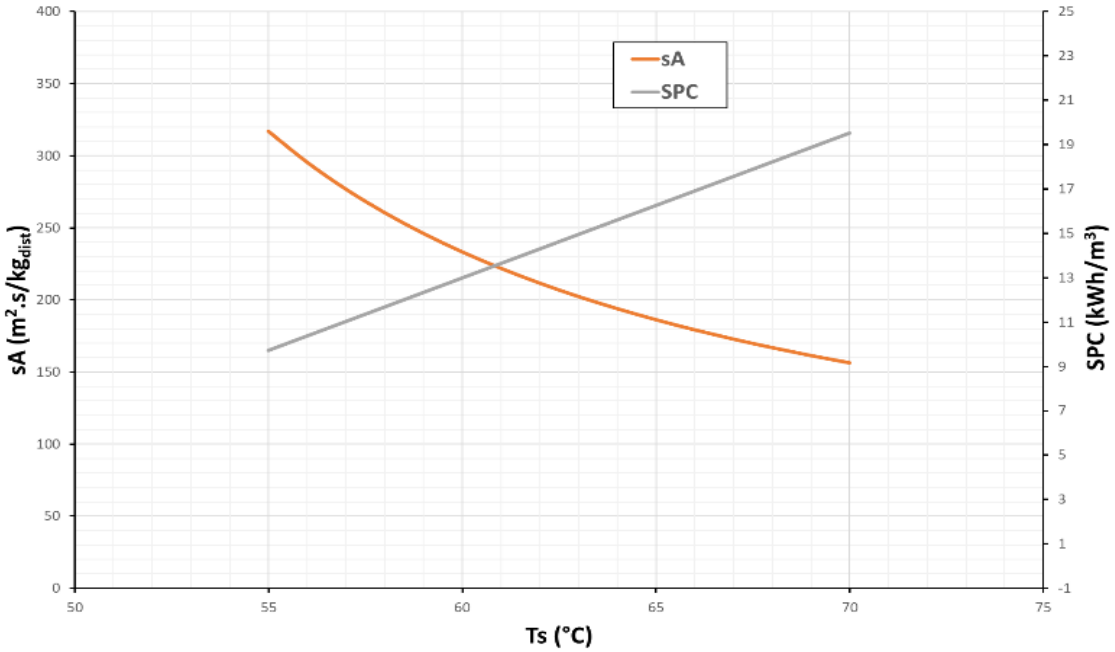

Figure 7. MED-MVC performance parameters with the heating steam saturation temperature.

The MED-MVC performance ratio decreases with increasing temperature due to the gradual increasing compressor power with distillate output kept constant and heating steam flowrate declining slightly, 3.08% between 55 and 70 °C. On the whole, the performance ratio of the entire system climbs up with rising temperature but very slowly due to two opposing effects: The first one is lower field size and consequently lower insolation and higher PR. The second one is the decrease in electricity output which causes lower PR, Fig. 8.

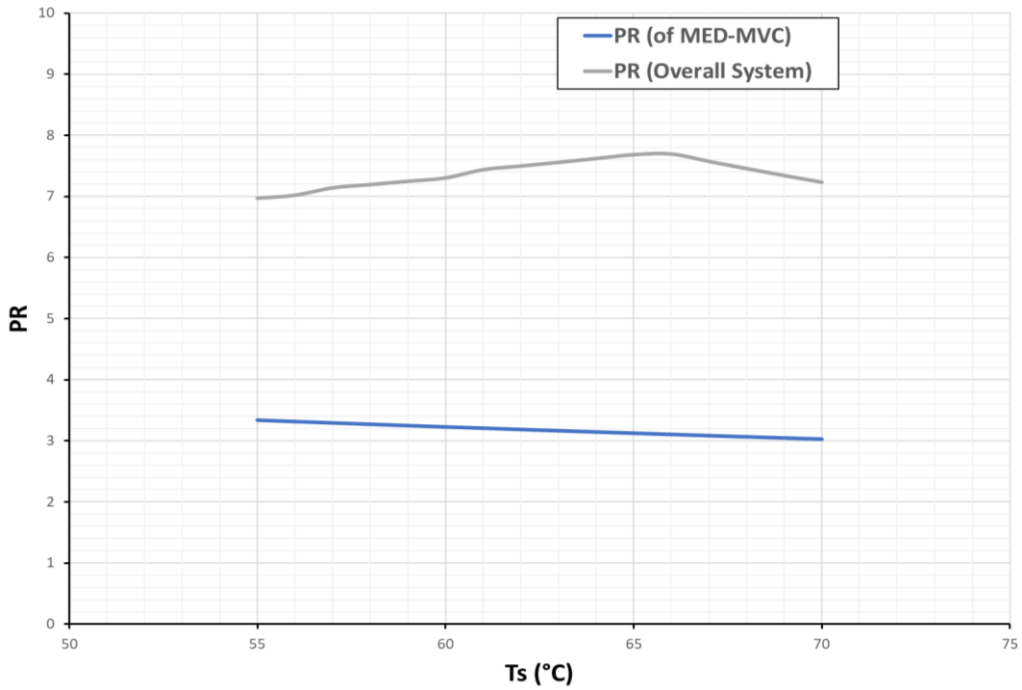

Figure 8. The performance ratio of the MED-MVC and the overall system trend with saturation temperature of heating steam.

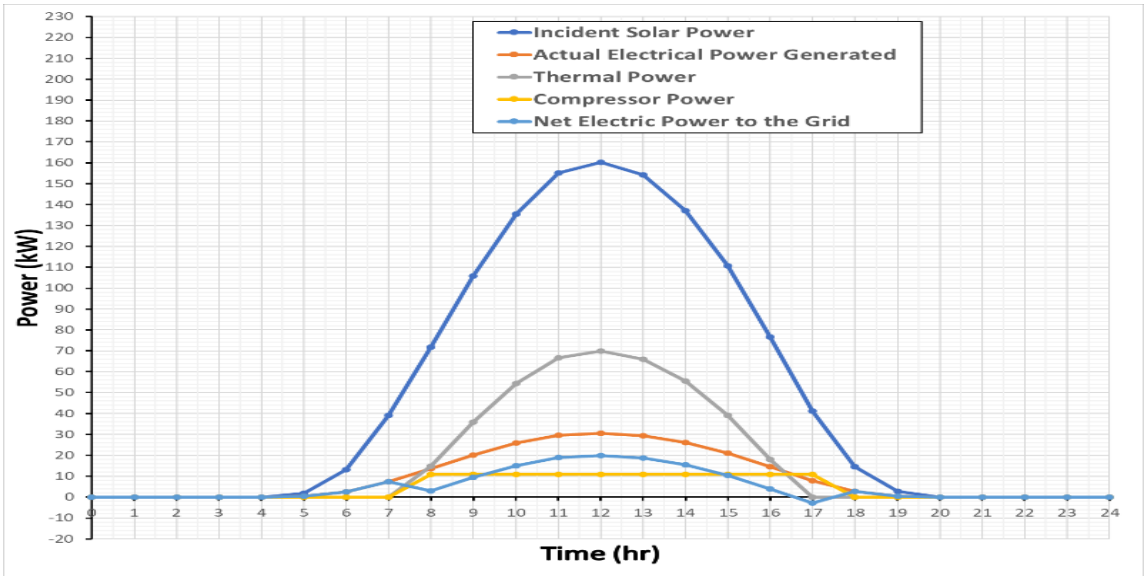

Figure 9. The system performance on the 21st of June in Alexandria, Egypt.

Furthermore, the system is tested for a typical day of summer, 21st June in Alexandria, Egypt. Hourly solar radiation data are extracted from PVSYST software. Hot water tank is designed to operate the system individually for 2 days of no sunlight. Heating steam saturation temperature is taken as 55 °C for better harnessing of solar thermal power. For normal operation, the system starts, when sun radiation is enough for positive thermal efficiency, generated is more than losses, then, the tank discharges for some hours till sun radiation is strong enough to power the system. After that, the tank charges and the system works simultaneously. The system performance is shown in Fig. 9. Volume of the tank is enlarged by a factor of 1.5 to accommodate further filling during the day and is guaranteed to reach its initial water capacity with an increase of 5% at the end of the day. Then, the system is stopped as depicted in Fig. 10.

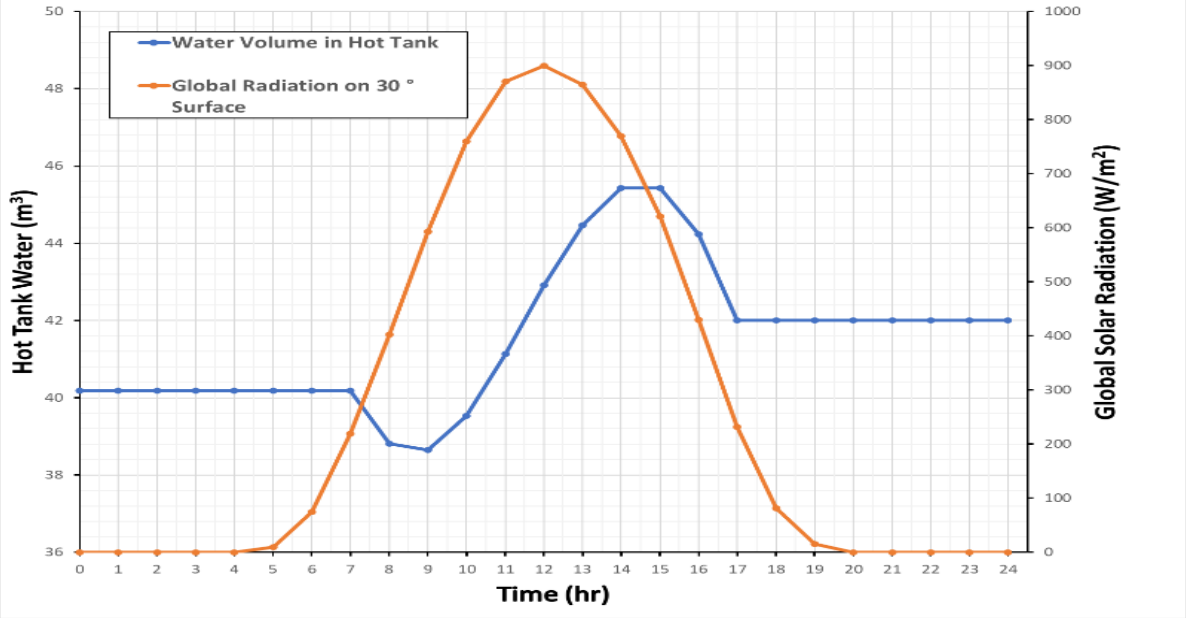

Figure 10. Storage tank charge/discharge curve with global incident solar radiation on 21st of June, Alexandria, Egypt.

The solar field is composed of 95 collectors and total freshwater production is 11.1 m^3, this is justified by the fact that average radiation during operation hours in that day is 690.11 W/m^2, which is larger than

the design value of 622 W/m^2, thereby the system works for extra hours. Thermal energy harnessed is 420.34 kWh, Net electricity to the grid is 136.11 kWh.

5. CONCLUSION

A multi-effect distillation system with mechanical vapor compression was designed to run by the thermal and electrical power of photovoltaic/thermal collectors. The solar field has been sized based on the required thermal energy of the desalination system for the weather conditions of Alexandria, Egypt. Produced electricity is used to power the compressor and the excess is injected into the grid. The main findings are as follows:

1) *Multi-effect distillation with mechanical vapor compression desalination system can be powered effectively by low temperature photovoltaic thermal collectors from energy perspective.*
2) *Heating steam saturation temperature has a significant impact on the compressor power, the thermal power requirements and the overall performance of the system. Elevating heating steam saturation temperature from 55 °C to 70 °C nearly halves the specific heat transfer area and doubles specific power consumption.*
3) *The overall performance of the system is enhanced by rising steam temperature until the overall produced power is consumed by the desalination system at 65 °C. Afterwhich, the system performance declines.*
4) *The required hot water storage capacity is large compared to the freshwater output due to utilization of sensible heat energy storage at relatively low temperature differences.*

In the future, an investigation of the best matching conditions between the desalination system and the PVT system can enhance performance. Besides, the utilization of latent heat energy storage can greatly reduce storage capacity required.

Acknowledgment

The authors express their appreciation to the Egyptian Ministry of Higher Education (MoHE) and the Egypt-Japan University of Science and Technology (E-JUST) for sponsoring and supporting this research.

REFERENCES

[1] Baniasad Askari, I, Ameri, M. A techno-economic review of multi effect desalination systems integrated with different solar thermal sources. *Applied Thermal Engineering* 2021; *185*: 116323, DOI: 10.1016/j.applthermaleng.2020.116323

[2] Yousef, MS, Hassan, H. Energy payback time, exergoeconomic and enviroeconomic analyses of using thermal energy storage system with a solar desalination system: An experimental study. *Journal of Cleaner Production* 2020; *270*: 122082, DOI: 10.1016/j.jclepro.2020.122082

[3] Bataineh, KM. Multi-effect desalination plant combined with thermal compressor driven by steam generated by solar energy. *Desalination* 2016; *385*: 39–52, DOI: 10.1016/j.desal.2016.02.011

[4] Shabgard, H, Xu, B, Parthasarathy, R. Solar thermal-driven multiple-effect thermosyphon distillation system for waste water treatment. In: Proceedings of ASME International Mechanical Engineering Congress and Exposition (IMECE), 3-9 November 2017: ASME, pp. 1–7.

[5] Alhaj, M, Mabrouk, A, Al-Ghamdi, SG. Energy efficient multi-effect distillation powered by a solar linear Fresnel collector. *Energy Conversion and Management* 2018; *171*: 576–586, DOI: 10.1016/j.enconman.2018.05.082

[6] Uğurlu, A, Gokcol, C. An overview of Turkey's renewable energy trend. *Journal of Energy Systems* 2017; *1*: 148–158, DOI: 10.30521/jes.361920
[7] Kim, YD, Thu, K, Myat, A, Ng, KC. Numerical simulation of solar-assisted multi-effect distillation (SMED) desalination systems. *Desalination and Water Treatment* 2013; *51*: 1242–1253, DOI: 10.1080/19443994.2012.695044
[8] Liu, X, Chen, W, Gu, M, Shen, S, Cao, G. Thermal and economic analyses of solar desalination system with evacuated tube collectors. *Solar Energy* 2013; *93*: 144–150, DOI: 10.1016/j.solener.2013.03.009
[9] Calise, F, Dentice d'Accadia, M, Piacentino, A. A novel solar trigeneration system integrating PVT (photovoltaic/thermal collectors) and SW (seawater) desalination: Dynamic simulation and economic assessment. *Energy* 2014; *67*: 129–148, DOI: 10.1016/j.energy.2013.12.060
[10] Zhang, Z, Hu, Z, Xu, H, Dai, X, Wang, J, Jiao, W, Yuan, Y, Phelan, P. Theoretical analysis of a solar-powered multi-effect distillation integrated with concentrating photovoltaic/thermal system. *Desalination* 2019; *468*: 114074, DOI: 10.1016/j.desal.2019.114074
[11] Alsehli, M, Alzahrani, M, Choi, JK. A novel design for solar integrated multi-effect distillation driven by sensible heat and alternate storage tanks. *Desalination* 2019; *468*: 114061, DOI: 10.1016/j.desal.2019.07.001
[12] Masoud Parsa, S, Majidniya, M, Alawee, WH, Dhahad, HA, Muhammad Ali, H, Afrand, M, Amidpour, M. Thermodynamic, economic, and sensitivity analysis of salt gradient solar pond (SGSP) integrated with a low-temperature multi effect desalination (MED): Case study, Iran. *Sustainable Energy Technologies and Assessments* 2021; *47*: 101478, DOI: 10.1016/j.seta.2021.101478
[13] Soliman, AM, Mabrouk, A, Eldean, MAS, Fath, HES. Techno-economic analysis of the impact of working fluids on the concentrated solar power combined with multi-effect distillation (Csp-med). *Desalination and Water Treatment* 2021; *210*: 1–21, DOI: 10.5004/dwt.2021.26566
[14] Naminezhad, A, Mehregan, M. Energy and exergy analyses of a hybrid system integrating solar-driven organic Rankine cycle, multi-effect distillation, and reverse osmosis desalination systems. *Renewable Energy* 2022; *185*: 888–903, DOI: 10.1016/j.renene.2021.12.076
[15] Karaca, G, Dolgun, EC, Kosan, M, Aktas, M. Photovoltaic-Thermal solar energy system design for dairy industry. *Journal of Energy Systems* 2019; *3*: 86–95, DOI: 10.30521/jes.565174
[16] Ortega-Delgado, B, García-Rodríguez, L, Alarcón-Padilla, DC. Opportunities of improvement of the MED seawater desalination process by pretreatments allowing high-temperature operation. *Desalination and Water Treatment* 2017; *97*: 94–108, DOI: 10.5004/dwt.2017.21679
[17] Sharqawy, MH, Lienhard V, JH, Zubair, SM. Thermophysical properties of seawater: A review of existing correlations and data. *Desalination and Water Treatment* 2010; *16*: 354–380, DOI: 10.5004/dwt.2010.1079
[18] Nayar, KG, Sharqawy, MH, Banchik, LD, Lienhard, JH. Thermophysical properties of seawater: A review and new correlations that include pressure dependence. *Desalination* 2016; *390*: 1–24, DOI: 10.1016/j.desal.2016.02.024
[19] El-Dessouky, H, Ettouney, H. Fundamentals of Salt Water Desalination. Amsterdam, NETHERLANDS: Elsevier 2002.
[20] El-Dessouky, H, Alatiqi, I, Bingulac, S, Ettouney, H. Steady-state analysis of the multiple effect evaporation desalination process. *Chemical Engineering and Technology* 1998; *21*: 437–451, DOI: 10.1002/(SICI)1521-4125(199805)21:5<437::AID-CEAT437>3.0.CO;2-D
[21] Nafey, AS, Fath, HES, Mabrouk, AA. Thermoeconomic design of a multi-effect evaporation mechanical vapor compression (MEE-MVC) desalination process. *Desalination* 2008; *230*: 1–15, DOI: 10.1016/j.desal.2007.08.021
[22] Elsayed, ML, Mesalhy, O, Mohammed, RH, Chow, LC. Performance modeling of MED-MVC systems: Exergy-economic analysis. *Energy* 2019; *166*: 552–568, DOI: 10.1016/j.energy.2018.10.080
[23] Shahzad, MW, Thu, K, Kim, Y deuk, Ng, KC. An experimental investigation on MEDAD hybrid desalination cycle. *Applied Energy* 2015; *148*: 273–281, DOI: 10.1016/j.apenergy.2015.03.062
[24] Buonomano, A, Calise, F, Palombo, A. Solar heating and cooling systems by absorption and adsorption chillers driven by stationary and concentrating photovoltaic/thermal solar collectors: Modelling and simulation. *Renewable and Sustainable Energy Reviews* 2018; *82*: 1874–1908, DOI:

10.1016/j.rser.2017.10.059
[25] Soliman, AMA, Hassan, H, Ookawara, S. An experimental study of the performance of the solar cell with heat sink cooling system. *Energy Procedia* 2019; *162*: 127–135, DOI: 10.1016/j.egypro.2019.04.014
[26] Gad, R, Mahmoud, H, Ookawara, S, Hassan, H. Energy, exergy, and economic assessment of thermal regulation of PV panel using hybrid heat pipe-phase change material cooling system. *Journal of Cleaner Production* 2022; *364*: 132489, DOI: 10.1016/j.jclepro.2022.132489